



Published in final edited form as:

Endocr Res. 2009 ; 34(1): 1–9. doi:10.1080/07435800902841280.

GNAS haploinsufficiency leads to subcutaneous tumor formation with collagen and elastin deposition and calcification

Akio Sakamoto^{1,2}, Antonius Plagge³, Michael Eckhaus³, Gavin Kelsey³, and Lee S Weinstein¹

¹*Metabolic Diseases Branch, National Institute of Diabetes and Digestive and Kidney Diseases, National Institutes of Health, Bethesda, Maryland, USA*

²*Department of Orthopaedic Surgery, Graduate School of Medical Sciences, Kyushu University, Fukuoka, Japan*

³*Laboratory of Developmental Genetics and Imprinting, the Babraham Institute, Cambridge, UK*

Abstract

The heterotrimeric G protein α -subunit $G_s\alpha$ links receptors to stimulation of cAMP/protein kinase A signaling, which inhibits skin fibroblast proliferation and collagen synthesis. We now describe the development of fibrous tumors in mice with heterozygous disruption of the *Gnas* gene, which encodes $G_s\alpha$ and other gene products. Disruption of *Gnas* exon 2 on either the maternal or paternal allele (*Gnas*^{E2-/+}) results in fibromas or angiofibromas on the ears, paws and tail beginning at 4 months of age. The tumors were composed of fibroblastic cell proliferation with collagen and elastin deposition and calcification, and seemed to be associated with mechanical skin damage. The presence of calcification was associated with greater amounts of matrix metalloproteinase-2, suggesting an association between calcium deposition and extracellular matrix degradation. Osteoblast-specific markers were absent, consistent with the calcification not being secondary to ossification. Molecular studies showed that the tumors were not associated with deletion of the wild-type allele, making it unlikely that these tumors resulted from homozygous loss of $G_s\alpha$. These findings provide *in vivo* evidence that $G_s\alpha$ pathways inhibit fibroblast and endothelial proliferation and matrix deposition.

Introduction

$G_s\alpha$ is a ubiquitously expressed G protein α -subunit that couples receptors to adenylyl cyclase and it is required for receptor-stimulated cAMP generation and protein kinase A (PKA) activation (14,15). $G_s\alpha$ is encoded by a complex imprinted gene (*GNAS* at 20q13 in humans, *Gnas* on mouse chromosome 2) that produces multiple gene products through the use of multiple alternative promoters and first exons that splice onto a common set of downstream exons (14,15). Heterozygous $G_s\alpha$ -inactivating mutations lead to Albright hereditary osteodystrophy (AHO), a syndrome characterized by short stature, skeletal and neurobehavioral defects and subcutaneous ossifications.

We previously generated mice with a mutation of *Gnas* exon 2 (*Gnas*^{E2-}) (16). While the homozygotes were embryonically lethal, the heterozygotes had distinct phenotypes associated with poor survival, and metabolic and neurological abnormalities depending on the parental origin of the mutation, due to the fact that $G_s\alpha$ is imprinted in a tissue-specific manner.

Address correspondence to: Akio Sakamoto, MD, PhD, 3-1-1 Maidashi, Higashi-ku, Fukuoka, 812-8582, Japan. Fax: +81-92-642-5507; E-mail: E-mail: akio@med.kyushu-u.ac.jp.

In the present report we describe a new feature of *Gnas*^{E2-/+} mice, namely the development of subcutaneous fibromas and angiofibromas on the ears, paws, and tail beginning at 4 months of age. Most of these tumors had collagen and elastin deposition with calcification, the latter being associated with the presence of increased matrix metalloproteinase-2 (MMP-2), an enzyme that has previously been shown to be associated with elastin degradation and vascular calcification (3). We also show that these tumors do not result from homozygous loss of *G_sα* due to somatic deletion of the wild-type allele.

Materials and Methods

Mice

Mice with heterozygous insertion of a neomycin resistance cassette within *Gnas* exon 2 (*Gnas*^{E2-/+}) were generated and maintained with a CD1 genetic background, as previously described (16). Animals were maintained on a 12-h light/dark cycle (6 am/6 pm) and a standard pellet diet (NIH-07, 5% fat by weight). Animal experiments were approved by the NIDDK Animal Care and Use Committee.

Histology

Dissected samples were fixed overnight in 4% paraformaldehyde, embedded in paraffin using standard procedures, and stained with hematoxylin and eosin, Masson-Trichrome, Elastica von Gieson, or von Kossa stains.

Immunohistochemistry

Sections were deparaffinized and rehydrated and endogenous peroxidase was blocked by methanol. The sections were incubated with antibodies for MMP-2 (R & D System, Inc. Minneapolis, MN, USA; 1:500), and for osteoblastic markers of osteopontin (Cosmo Bio Co., Ltd., Tokyo, Japan; 1:300) and bone sialoprotein (Cosmo Bio Co., Ltd., Tokyo, Japan; 1:300) at 4°C overnight, followed by reaction with the streptavidin-biotin complex method using the SAB-PO kit (Nichirei, Tokyo, Japan). The sections were then reacted in a 3,3'-diaminobenzidine, peroxytrichloride substrate solution, counterstained with hematoxylin, and then mounted.

Analysis for allelic loss of *Gnas*

DNA was extracted from 30- μ m paraffin-embedded tissue sections in which the tumor occupied more than 80% of the total section area. Paraffin was removed with xylene, and the sample was then washed twice with 100% ethanol and subsequently dried. Genomic DNA was then extracted using a DNA extraction kit (DNeasy Tissue Kit, Qiagen, Germantown, MD, USA). DNA fragments (1 μ l) were amplified by PCR in 25 μ l reactions consisting of 2.5 μ l PCR buffer and 0.1 μ l Taq polymerase (Ex Taq, Takara Bio Inc., Kyoto, Japan) with 6 μ l betaine (Sigma, St Louis, MI, USA). PCR reactions included a common upstream primer (F1: 5'-CCCACGCCCTCACTTTCCTT-3'), and two downstream primers complementary to *G_sα* wild type sequence (R2E2: 5'-ACCACCTGTCCTGCTCAGTG-3' and Neo sequence (R4neo: 5'-GCAGGGGCCCTATAACTT CG-3'). In the presence of the F1 upstream primer, the downstream primers R2E2 and R4neo amplify PCR products from the wild-type (142 bp) and mutant (130 bp) alleles, respectively. The PCR cycling profile included an initial denaturation at 94°C for 5 min, followed by 36 cycles of annealing (58°C, 30 s), extension (72°C, 1 min), and denaturation (94°C, 30 s) and a final cycle with a 7 min extension. Products were assessed by acrylamide gel electrophoresis and ethidium bromide staining..

Results

Gnas^{E2-/+} mice developed round, smooth, protuberant nodules on the ears, paws and tail (Fig. 1A, 1C). These areas are more prone to skin damage and in some cases skin damage was evident in the vicinity of the nodules. These nodules first appeared at 4 months of age and their frequency increased steadily over time, with the result that they were present in all mutants that were over 400 days of age (Fig. 1D). No nodules were observed in control littermates. These tumors were present regardless of whether the mutation was maternally or paternally inherited. X-rays revealed that most of the tumors had calcification (Fig. 1B).

Histological evaluation showed that these tumors were confined to subcutaneous tissue with no involvement of deeper tissues. Lesions showed proliferation of fibroblasts in fascicles with variable amounts of collagenous matrix, features consistent with fibroma (Fig. 2A, D). In many tumors, massive myxoid matrix was also observed (Fig. 2B). Some tumors also showed increased blood vessel formation, consistent with angiofibroma (Fig. 2C). There were no clear borders between the tumor and normal tissue. Tumors typically had a dense collagenous matrix (Figs. 2D, 3A) with the presence of elastin deposition (Fig. 3B) and calcification (Fig. 3C). Cells embedded within calcified matrix showed strong positive staining for MMP-2 (Fig. 3D). These results suggest that fibroblasts having collagen with calcification matrix seen in E2KO are a result of abnormal matrix remodeling. No features characteristic of bone formation were present and immunohistochemical staining for osteopontin and bone sialoprotein was negative (data not shown), confirming that the calcification is not the result of ossification.

The presence of tumors in mice with disruption of either the maternal or paternal *Gnas* allele suggests that these tumors are probably the result of *G_sα* haploinsufficiency rather than total *G_sα* deficiency due to the combined effects of the mutation of one allele and the imprinting of the other allele. To rule out the possibility that the tumors result from somatic deletion of the wild-type allele leading to total *G_sα* deficiency, we performed duplex PCR on control and tumor genomic DNA samples to determine whether the wild-type allele was lost. The PCR reactions showed a common upstream primer located within intron 1 and two downstream primers, one with the wild-type exon 2 sequence and the second with a sequence within the neomycin cassette (Neo). These two downstream primers lead to amplification of a 142-bp band from the wild-type allele and a 130-bp band from the mutant allele. Amplification of three controls (wild-type ear tissue) resulted in a single 142-bp wild-type band (Fig. 4), while amplification of 9 tumor samples (Fig. 4 and data not shown) showed equal amplification of both the wild-type and mutant bands, consistent with no loss of the wild-type allele in these tumor samples. Of course, this experiment does not rule out the presence of other small mutations and deletions within the wild-type allele.

Discussion

GNAS-activating mutations, also known as the *gsp* oncogene, are associated with endocrine tumors, skeletal muscle myxomas, and fibrous dysplasia of bone. On the other hand, *GNAS*-inactivating mutations in AHO patients are not associated with neoplasms (14,15). In this study we show that, over time, mice with *Gnas*-inactivating mutations develop subcutaneous fibrotic lesions that have the histological features of fibroma or angiofibroma which is associated with various density of collagenous matrix. These tumors only develop at the ears, paws and tail where the skin can be injured mechanically and therefore the development of these lesions may result from a repair reaction leading to the proliferation of fibroblasts.

Whether or not the tumors we observe are clonal or hyperplastic is not clear. Our results show no evidence for loss of the unaffected *Gnas* allele in our tumor samples, indicating that these tumors are not the result of a 'second hit' of the normal allele as is typical of classical tumor

suppressor genes. Since tumors were present in both types of mice with disruption of the maternal and paternal *Gnas* allele, the tumors did not arise as a result of total $G_s\alpha$ deficiency due to mutation of one allele and imprinting of the other. This is consistent with a previous study in humans showing that $G_s\alpha$ is not imprinted in skin (7).

Previous studies reported that activation of the $G_s\alpha$ /PKA pathway leads to increased apoptosis and differentiation and decreased proliferation of endothelial cells (5) and vascular smooth muscle cells (4,6). Moreover, the role of PKA in normal and hypertrophic scar fibroblasts was highlighted in a study showing that IFN- γ transiently inhibited proliferation and collagen synthesis by activating PKA (17). These findings predict that a genetic lesion leading to reduced $G_s\alpha$ /PKA would result in increased skin fibroblast proliferation and collagen synthesis. The presence of fibrotic tumors in *Gnas*^{E2-/+} mice provides *in vivo* evidence that insufficient $G_s\alpha$ /PKA signaling leads to abnormal proliferation of skin fibroblasts.

The tumors in *Gnas*^{E2-/+} mice are associated with increased collagen deposit. $G_s\alpha$ /PKA activation leads to reduced inhibited collagen synthesis in endothelial cells (5) and fibroblasts (17). Therefore, it is possible that excess collagen synthesis occurs at the ears, paws and tail during the repair process as a result of decreased $G_s\alpha$ /PKA signaling. Increased collagen may also be the result of reduced collagen degradation. MMPs, including MMP-2, have a specialized role to play in the turnover of the extracellular matrix during many normal tissue processes, such as wound healing, bone resorption and morphogenesis (9,12). One prior study showed no effects of cAMP analogs on MMP-2 expression (18), while another study showed that cAMP/PKA stimulates MMP-2 (13). The role of partially reduced cAMP/PKA signaling on the rate of collagen degradation in the tumors of *Gnas*^{E2/-} mice remains to be determined.

Ectopic calcification is an important component of disorders which contributes to clinically significant sequelae, such as valvular disease and atherosclerosis. In these affected tissues elastin is the predominant extracellular matrix component and it is responsible for elastic recoil of the aorta, heart valve cusps and arterial walls (11). In these tissues elastin also plays a role in the process of calcification. Elastin deposition and ectopic calcification were also both observed in tumors from *Gnas*^{E2-/+} mice, and increased MMP-2 expression was present in cells in the vicinity of the calcifications. A correlation between MMP-mediated elastin degradation and vascular calcification has been reported (3). MMP-2 binds to and digests insoluble elastin (8), and has been shown to be actively involved in elastin degradation (2,10). It has been suggested that MMP-mediated elastin degradation leads to formation of soluble elastin peptides, which may influence cellular activity towards promoting calcium deposition (1).

Tumors reminiscent of those observed in *Gnas*^{E2-/+} mice are not a feature of AHO (14,15). However AHO patients do develop subcutaneous ossifications (osteoma cutis or progressive osseous heteroplasia). The lesions we observe in *Gnas*^{E2-/+} mice do not resemble those seen in AHO patients. In AHO patients, ossifications occur at a very young age while in mice the tumors occur later in life. Moreover the lesions in AHO patients result are primarily the result of intramembranous ossification, whereas the lesions in mice do not result from ossification. Rather, the calcification in the mouse tumors appears to be a secondary calcification of a fibrotic lesion. Therefore, the mechanism of calcification in AHO and that in *Gnas*^{E2-/+} mouse tumors appear to be very different. The *Gnas*^{E2-/+} mouse may be a useful model for further studies on the mechanism of skin fibroblast proliferation and calcification.

Acknowledgement

This work was supported by the Intramural Research Program of the National Institute of Diabetes and Digestive and Kidney Diseases, National Institutes of Health.

References

1. Bailey M, Pillarisetti S, Jones P, Xiao H, Simionescu D, Vyavahare N. Involvement of matrix metalloproteinases and tenascin-C in elastin calcification. *Cardiovasc Pathol* 2004;13:146–155. [PubMed: 15081471]
2. Bailey M, Xiao H, Ogle M, Vyavahare N. Aluminum chloride pretreatment of elastin inhibits elastolysis by matrix metalloproteinases and leads to inhibition of elastin-oriented calcification. *Am J Pathol* 2001;159:1981–1986. [PubMed: 11733347]
3. Basalyga DM, Simionescu DT, Xiong W, Baxter BT, Starcher BC, Vyavahare NR. Elastin degradation and calcification in an abdominal aorta injury model: role of matrix metalloproteinases. *Circulation* 2004;110:3480–3487. [PubMed: 15545515]
4. Chen YM, Wu KD, Tsai TJ, Hsieh BS. Pentoxifylline inhibits PDGF-induced proliferation of and TGF-beta-stimulated collagen synthesis by vascular smooth muscle cells. *J Mol Cell Cardiol* 1999;31:773–783. [PubMed: 10329205]
5. D'Angelo G, Lee H, Weiner RI. cAMP-dependent protein kinase inhibits the mitogenic action of vascular endothelial growth factor and fibroblast growth factor in capillary endothelial cells by blocking Raf activation. *Journal of Cellular Biochemistry* 1997;67:353–366. [PubMed: 9361190]
6. Graves LM, Bornfeldt KE, Sidhu JS, Argast GM, Raines EW, Ross R, Leslie CC, Krebs EG. Platelet-derived growth factor stimulates protein kinase A through a mitogen-activated protein kinase-dependent pathway in human arterial smooth muscle cells. *J Biol Chem* 1996;271:505–511. [PubMed: 8550611]
7. Mantovani G, Bondioni S, Locatelli M, Pedroni C, Lania AG, Ferrante E, Filopanti M, Beck-Peccoz P, Spada A. Biallelic expression of the Gsalpha gene in human bone and adipose tissue. *J Clin Endocrinol Metab* 2004;89:6316–6319. [PubMed: 15579796]
8. Mecham RP, Broekelmann TJ, Fliszar CJ, Shapiro SD, Welgus HG, Senior RM. Elastin degradation by matrix metalloproteinases. Cleavage site specificity and mechanisms of elastolysis. *J Biol Chem* 1997;272:18071–18076. [PubMed: 9218437]
9. Nagase H, Woessner JF Jr. Matrix metalloproteinases. *J Biol Chem* 1999;274:21491–21494. [PubMed: 10419448]
10. Okada Y, Katsuda S, Okada Y, Nakanishi I. An elastinolytic enzyme detected in the culture medium of human arterial smooth muscle cells. *Cell Biol Int* 1993;17:863–869. [PubMed: 8220313]
11. Robert L, Jacob MP, Fulop T. Elastin in blood vessels. *Ciba Found Symp* 1995;192:286–299. [PubMed: 8575262]
12. Sternlicht MD, Werb Z. How matrix metalloproteinases regulate cell behavior. *Annu Rev Cell Dev Biol* 2001;17:463–516. [PubMed: 11687497]
13. Tsuruda T, Kato J, Cao YN, Hatakeyama K, Masuyama H, Imamura T, Kitamura K, Asada Y, Eto T. Adrenomedullin induces matrix metalloproteinase-2 activity in rat aortic adventitial fibroblasts. *Biochem Biophys Res Commun* 2004;325:80–84. [PubMed: 15522203]
14. Weinstein, LS. GNAS and McCune-Albright syndrome/fibrous dysplasia, Albright hereditary osteodystrophy/pseudohypoparathyroidism type 1A, progressive osseous heteroplasia, and pseudohypoparathyroidism type 1B. Epstein, CJER.; Wynshaw-Boris, A., editors. Oxford University Press; San Francisco: 2004. p. 849-866.
15. Weinstein LS, Yu S, Warner DR, Liu J. Endocrine manifestations of stimulatory G protein alpha-subunit mutations and the role of genomic imprinting. *Endocr Rev* 2001;22:675–705. [PubMed: 11588148]
16. Yu S, Yu D, Lee E, Eckhaus M, Lee R, Corria Z, Accili D, Westphal H, Weinstein LS. Variable and tissue-specific hormone resistance in heterotrimeric Gs protein alpha-subunit (Gsalpha) knockout mice is due to tissue-specific imprinting of the gsalpha gene. *Proc Natl Acad Sci USA* 1998;95:8715–8720. [PubMed: 9671744]
17. Zhang XF, Guo SZ, Lu KH, Li HY, Li XD, Zhang LX, Yang L. Different roles of PKC and PKA in effect of interferon-gamma on proliferation and collagen synthesis of fibroblasts. *Acta Pharmacol Sin* 2004;25:1320–1326. [PubMed: 15456534]

18. Zhong ZD, Hammani K, Bae WS, DeClerck YA. NF-Y and Sp1 cooperate for the transcriptional activation and cAMP response of human tissue inhibitor of metalloproteinases-2. *J Biol Chem* 2000;275:18602–18610. [PubMed: 10764764]

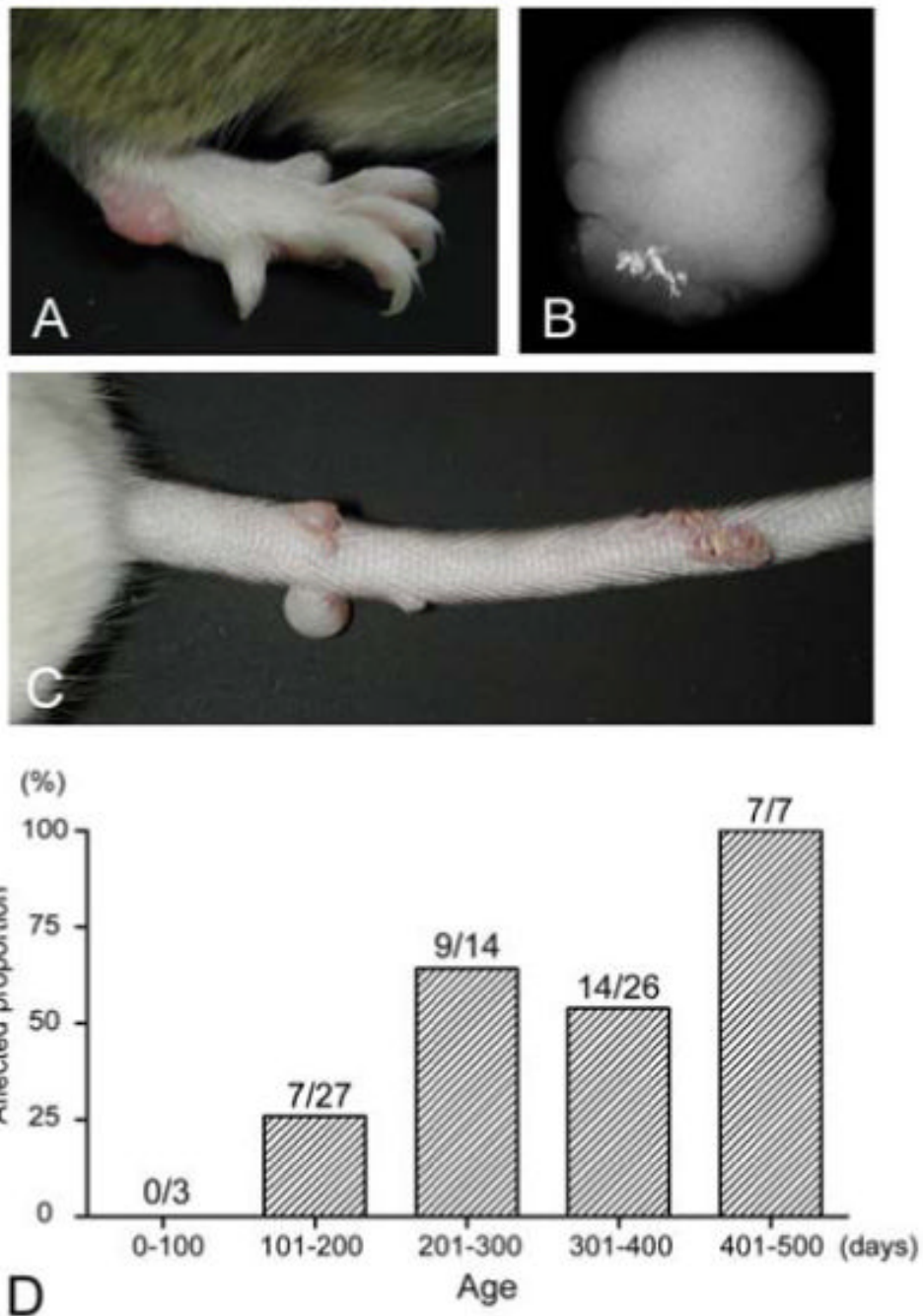


Figure 1. Subcutaneous nodules in *Gnas*^{E2-/+} mice. Photographs of protuberant nodules on the (A) paw and (B) tail of a *Gnas*^{E2-/+} mouse. (C) Radiograph of one tumor showing calcification. (D) Frequency of *Gnas*^{E2-/+} mice with subcutaneous nodules as a function of age in days.

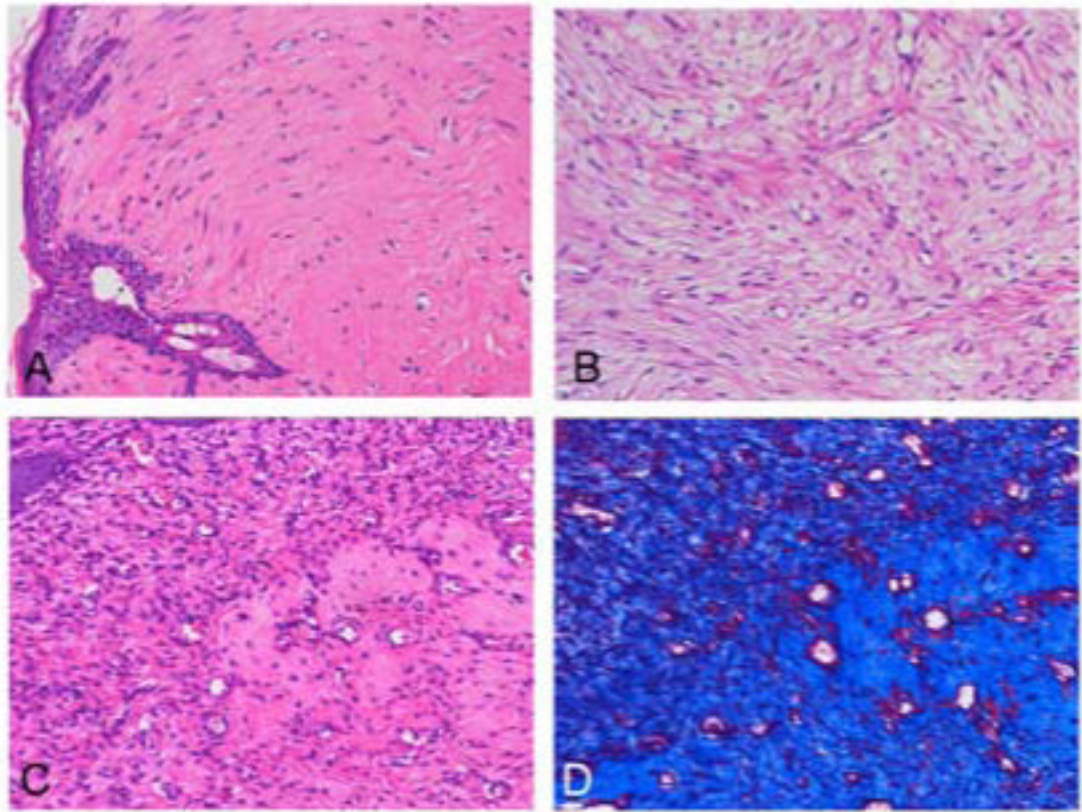


Figure 2.

Histology of tumors in *Gnas*^{E2-/-} mice. (A) Section of a tumor showing fibroblast proliferation with typical collagen matrix consistent with fibroma. (B) Tumor with myxoid matrix. (C) Tumor with increased fibroblast proliferation and blood vessel formation, consistent with angiofibroma. (D) Masson-Trichrome staining showing massive collagen deposition. (A-C stained with hematoxylin and eosin).

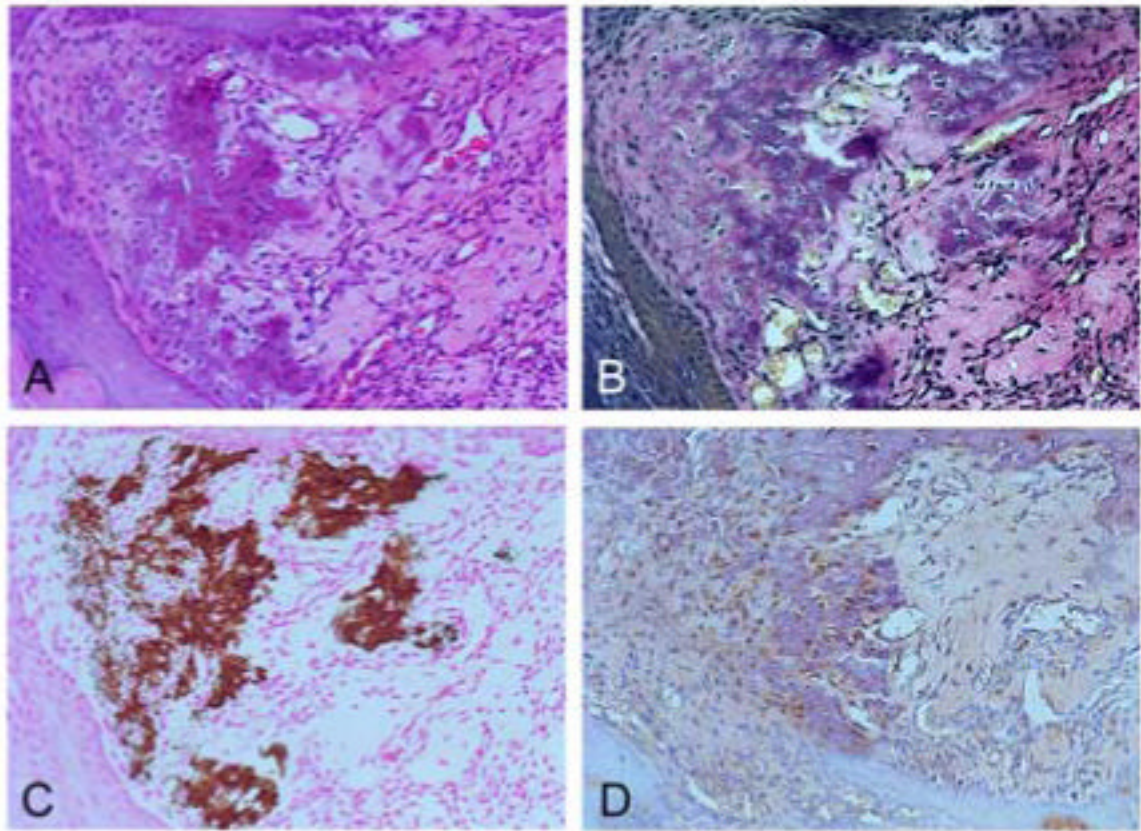
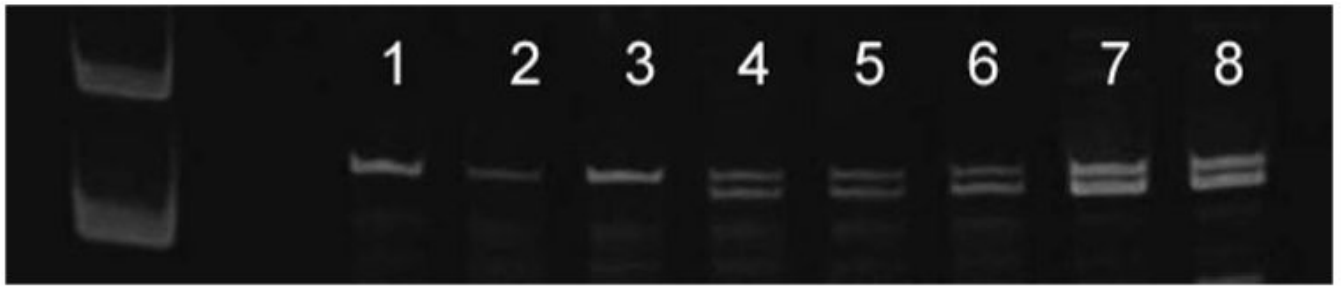


Figure 3. Collagen and elastin deposition and calcification in tumors Sections of a tumor stained with (A) hematoxylin and eosin stain, showing collagen deposition; (B) Elastica von Gieson stain, showing elastin deposition (black); and (C) von Kossa staining, showing calcification. (D) Immunohistochemistry with an anti-MMP-2 antibody, showing strong MMP-2 staining within cells embedded in collagen with calcification.

**Figure 4.**

Genetic analysis of tumor DNA samples for deletion of wild-type *Gnas* allele. Duplex PCR analysis of genomic DNA from 3 control samples (wild-type ear, lanes 1-3) and 5 tumors (lanes 4-8) was performed to amplify bands from wild-type (142 bp) and mutant (130 bp) alleles. Controls only amplified the 142-bp wild-type band, while all tumors amplified both wild-type and mutant bands, consistent with the presence of both alleles.